Charting Disease Trajectories from Isolated REM Sleep Behavior Disorder to Parkinson's Disease

Cécile Di Folco, Raphaël Couronné, Isabelle Arnulf, Graziella Mangone, Smaranda Leu-Semenescu, Pauline Dodet, Marie Vidailhet, Jean-christophe Corvol, Stéphane Lehéricy, Stanley Durrleman

Charting disease trajectories from isolated REM sleep behavior disorder to Parkinson's disease

Cécile Di Folco, Msc[1-6,*], Raphaël Couronné, PhD[1-6,*], Isabelle Arnulf, MD, PhD[2-6], Graziella Mangone, MD, PhD[2-6], Smaranda Leu-Semenescu, MD[2-6], Pauline Dodet, MD[2-6], Marie Vidailhet, MD, PhD[2-6], Jean-Christophe Corvol, MD, PhD[2-6,*], Stéphane Lehéricy, MD, PhD[2-6,*] and Stanley Durrleman, PhD[1-6]

* equal contributions

Abstract

Background: Clinical presentation and progression dynamics are variable in patients with Parkinson's disease (PD). Disease course mapping is an innovative disease modelling technique that summarizes the range of possible disease trajectories, and estimates dimensions related to onset, sequence, and speed of progression of disease markers.

Objective: To propose a disease course map for PD and investigate progression profiles in patients with or without rapid eye movement sleep behavioral disorders (RBD).

Methods: Data of 919 PD patients and 88 isolated RBD patients from three independent longitudinal cohorts were analyzed (follow-up duration = 5.1 (1.1, 8.1) years (95% CI)). Disease course map were estimated by using eight clinical markers (motor and non-motor symptoms) and four imaging markers (dopaminergic denervation).

Results: PD course map showed that the first changes occurred in the contralateral putamen 13 years before diagnosis, followed by changes in motor symptoms, dysautonomia, sleep – all before diagnosis – and finally cognitive decline at the time of diagnosis. The model showed

earlier disease onset, earlier non-motor and later motor symptoms, more rapid progression of cognitive decline in PD patients with RBD than PD patients without RBD. This pattern was even more pronounced in patients with isolated RBD with early changes in sleep, followed by cognition and non-motor symptoms and later changes in motor symptoms.
Conclusions: Our findings are consistent with the presence of distinct patterns of progression between patients with and without RBD. Understanding heterogeneity of PD progression is key to decipher the underlying pathophysiology and select homogeneous subgroups of patients for precision medicine.

Conflict of Interest

IA has served in the speaker bureau for UCB Pharma and as a consultant for Idorsia Pharma. SLS has received funds for travel to conferences from UCB Pharma. SL was awarded a research grant from Biogen Inc and has acted as a consultant for Roche. JCC has served on advisory boards for Biogen, Denali, Idorsia, Prevail Therapeutic, Theranexus, UCB, and received grants from Sanofi and the Michael J Fox Foundation outside this work. PD has received funds from UCB and Roche. SD has received grants from Sanofi and is co-inventor of the patent "a method for determining the temporal progression of a biological phenomenon and associated methods and devices" under reference WO/2017/194995. Other authors do not declare competing interests.

Funding

This research was funded in part by the *European Research Council* (ERC) under grant agreement No. 678304, the European Union's Horizon 2020 research and innovation programme under grant agreement No. 826421 (TVB-Cloud), *Agence Nationale de la*

Recherche (ANR) under grant agreements ANR-10-IAIHU-06 (IHU ICM), ANR-11-INBS-0006, ANR-19-P3IA-0001 (PRAIRIE Institute), ANR-19-JPW2-000 (JPND E-DADS), ANR-21-JPW2-0005-05 (JPND CONTROL-PD); *association France Parkinson* (PRECISE-PD project), the *Fondation d'Entreprise EDF*, Biogen Inc., *Fondation Thérèse and René Planiol*, *Fondation Saint Michel*. The work received unrestricted support for Research on Parkinson's disease from Energipole (M. Mallart), M. Villain and the *Société Française de Médecine Esthétique* (M. Legrand).

Author affiliations:

1 Inria, Centre de Paris, Paris, France

2 Paris Brain Institute – ICM, F-75013, Paris, France

3 Inserm, U 1127, Paris, France

4 CNRS, UMR 7225, Paris, France

5 Sorbonne Université, Paris, France

6 AP-HP, Hôpital de la Pitié Salpêtrière, Paris, France

Correspondence to: Stanley Durrleman

Full address: ICM, 47 Boulevard de l'Hôpital, 75013, Paris

E-mail: Stanley.Durrleman@inria.fr

Running title: Disease trajectories in Parkinson's disease

Keywords: Parkinson’s disease; REM sleep behavior disorder; Longitudinal data; Disease modelling

Abbreviations: Drug interaction with genes in Parkinson's disease = DIGPD; Cohort Study to Identify Predictive Factors for the Onset and Progression of Parkinson's Disease = ICEBERG; isolated rapid eye movement sleep behavior disorder = iRBD; Movement Disorder Society Unified Parkinson’s Disease Rating Scale = MDS-UPDRS; Mini-Mental State Examination = MMSE; Montreal Cognitive Assessment = MoCA; parkinsonian age = PA; Parkinson’s disease = PD; Parkinson’s disease with rapid eye movement sleep behavior disorder = PDRBD+; Parkinson’s disease without rapid eye movement sleep behavior disorder = PDRBD-; Parkinson’s Progression Markers Initiative = PPMI; rapid eye movement sleep behavior disorder = RBD; REM Sleep Behavior Disorder Screening Questionnaire = RBDSQ; Scales for Outcomes in Parkinson’s Disease - Autonomic Dysfunction = SCOPA-AUT; striatal binding ratio = SBR.

Introduction

Parkinson's disease (PD) has a long prodromal phase during which neuropathological (1) and clinical (2) changes develop slowly. It is commonly accepted that the progressive onset of motor and non-motor symptoms in PD is secondary to the sequence of brain functional and anatomical alterations. The most influential model describing this prodromal phase, based on neuropathology (1), does not fully explain the considerable heterogeneity of disease presentation (3–5). Increasing evidence suggests that the sequence and timing of clinical and imaging abnormalities vary considerably between patients.

The description and prediction of individual disease trajectories is important to personalize patient care, select more homogeneous sets of patients for clinical trials or contrast post-intervention outcomes with the natural course of the disease (6,7). The general approach is to cluster patient data at baseline, and then show that the rates of change in biomarker levels differ significantly between clusters (8–12). Such methods have successfully been used to define stereotypic progression profiles, such as a motor-predominant less severe form of the disease relative to a diffuse severe 'malignant' form with greater cognitive impairment, rapid eye movement sleep behavioral disorders (RBD), and dysautonomia (13). However, the assignment of a patient to a particular subtype is questionable, because patients may go through different disease states (14). Progression may be better described as a patient-specific sequence of events (15), and subtypes are probably overlapping entities within a multidimensional spectrum (16,17). These approaches aim to summarize heterogeneity in the clinical presentation of the disease, but they provide little information about the differences in progression dynamics.

Disease course mapping is a disease modeling technique that summarizes the range of possible disease trajectories by positioning the progression of each patient relative to a reference population in several dimensions (18,19). Disease course mapping estimates parameters at the individual level, which measures differences in the dynamics of progression (age at onset and speed of progression) and disease presentation (the relative values of the various biomarkers at a given disease stage). We applied here this novel statistical learning technique for the first time in PD after showing that it predicts specific progression profiles in patients with Alzheimer's and Huntington diseases (20,21). We propose a disease course map based on a set of clinical and brain imaging markers extracted from three independent longitudinal cohorts of PD patients. We used this approach to compare the trajectories of PD patients with and without RBD, previously shown to have different progression profiles (22,23). We finally compared these disease course maps to that of patients with isolated RBD, thought to be a good model of the premotor phase of the disease (24).

Materials and methods

Materials

Participants

We used data from three independent longitudinal studies: 1) the Parkinson's Progression Markers Initiative (PPMI, https://www.ppmi-info.org), as of February 2020, 2) DIGPD(25), a French 5-year longitudinal multicenter study in early PD and 3) ICEBERG a 5-year longitudinal single-center study in PD, iRBD, and healthy controls conducted at the Paris Brain Institute (ICM) (https://clinicaltrials.gov/ct2/show/NCT02305147), as of January 2021. From

these cohorts, we included available data from patients with idiopathic PD, iRBD, and healthy controls.

Definition of RBD status

The status of iRBD patients from PPMI and ICEBERG were based on video-polysomnography (VPG). For PD patients, VPG not being available in the three cohorts, we defined two subgroups according to the presence (PDRBD+) or absence (PDRBD-) of probable RBD based on clinical diagnosis. PDRBD+ was defined as a score $\geq$ 6 on the RBD screening questionnaire (RBDSQ)(26) over the course of the disease in PPMI, a score of $\geq$ 18 on the Honk-Kong version of the RBDSQ in ICEBERG, and the diagnosis reported by the clinician in DIGPD. In ICEBERG cohort where VPG was available, patients with discordant diagnosis between RBDSQ and VPG were excluded from the analysis. PD patients not fulfilling these criteria were considered PDRBD-.

Clinical and brain imaging markers

Clinical markers used for our models were scores at each visit of the:

- Movement Disorders Society-Unified Parkinson's Disease Rating Scale (MDS-UPDRS) part I, II, III in off or on states,
- Scale for Outcomes in Parkinson disease – Autonomic Dysfunction subscale (SCOPA-AUT),
- Montreal Cognitive Assessment (MoCA),
- Mini-Mental State Examination (MMSE),
- RBDSQ.

Brain imaging markers were striatal binding ratios (SBR) provided in the PPMI dataset for the putamen (Put.) and caudate nucleus (Caud.) measured by dopamine transporter scans of the ipsi- (Ipsi) or contralateral (Contra) hemisphere.

We reversed markers that decreased with progression so that all markers increase over the course of the disease. We normalized markers to a scale between 0 (normal value) and 1 (maximum pathological change). For the clinical markers of all cohorts, normal values and maximum pathological changes corresponded to their theoretical maximum and minimum values. For imaging markers, we defined the normal value as the mean SBR of controls at baseline, and the maximum pathological change as a SBR of 0.

Statistical analysis

Participants characteristics

Data are described as means ± standard deviation. Comparison between cohorts and subgroups were performed by using ANOVA (parametric) or Kruskal-Wallis (non-parametric) tests followed by *t*-tests or Mann-Whitney *U* tests, respectively. Significance was set at $p<0.05$.

Disease course mapping

Disease course mapping uses a longitudinal data set with a series of markers(19). It estimates the average progression in the form of a series of logistic curves starting from the value corresponding to a healthy state and ending at the maximum pathological change. Three series of parameters changed the relative shape and position of these curves to account for phenotypic differences between patients and variations in progression (see Supplementary Fig. 1):

- An intermarker spacing for each marker, showing how early (negative intermarker spacing) or late (positive intermarker spacing) the onset of the marker is relative to other markers (Supplementary Fig. 1B).
- A time-shift corresponding to the earliness (negative time-shift) or lateness (positive negative-shift) of disease onset compared to that of the population, taking all markers into account (Supplementary Fig. 1C).
- An acceleration factor corresponding to the fast (factor greater than 1) or slow (factor smaller than 1) speed of progression compared to that of the population, taking all markers into account (Supplementary Fig. 1D).

The Parkinsonian age (PA) is the time index of the set of logistic curves. It represents the age of the theoretical most typical patient in the population and can be understood therefore as a continuous disease staging scale. The chronological age of a patient at a given visit is mapped to one PA using the patient time-shift and acceleration factor, using an affine transform. Two different subjects that are observed at the same disease stage will thus have the same PA but a different chronological age. For an acceleration factor of 2, the duration between two consecutive visits of the patient is twice longer than between the corresponding PA. On average in the population, one year in the PA axis corresponds to one year in chronological age. By contrast, the intermarker spacing does not change the PA of the patient: these variables change the disease presentation of the patient at a given disease stage.

We estimated the disease course map with a non-linear Bayesian mixed-effects model in which the shape and position of the logistics curves represented the fixed effects and the patient individual parameters (intermarker spacings, time-shift, and acceleration factor) the random effects.

PD course map estimation did not require data to be sampled at regular time points or uniform sampling across patients. Disease course mapping does not require imputation for missing data since the model likelihood is informed using available data only. The estimation of the model parameters was shown to be robust to missing data (27). If one biomarker is missing for one subject, the values of the other observed biomarkers drive the estimation of the time-shift and acceleration factor, these two variables influencing the dynamics of all biomarkers in the same way. The inter-marker spacing for this biomarker is inferred from the pattern that the set of inter-marker spacing forms at the population level. The model estimates this pattern during the training procedure by analyzing the relationships among intermarker spacings: it does not require all biomarkers to be observed in all patients, but overlapping sub-sets of biomarkers for different patients.

Disease course mapping has several distinctive characteristics in contrast to usual linear mixed models for longitudinal analysis. First, it accounts for the non-linear dynamics of biomarker changes across disease progression stages. The model maps the short-term data of patients at different disease stages to different portions of a curve that depicts a long-term non-linear scenario of change. Second, linear mixed models have two random effects: the slope and the intercept. The intercept captures the variations of the biomarker values at a given time-point. Such models require therefore that patients are re-aligned in time with respect to a reference time-point, taken as the age at diagnosis or age at baseline for instance. They assume therefore that patients at the chosen reference time-point are at the same disease stage. Several previous works that model individual disease trajectories make such an assumption, whether within a linear (28,29) or non-linear framework (30). By contrast, disease course mapping replaces the intercept by the time-shift, thus capturing the variations in the patients' age at which the

biomarker reaches different levels. It uniquely positions the observed progression along two independent axes: early/late and fast/slow progression.

PD Course Maps

We built two PD Course Maps:

- A multimodal course map using both clinical (MDS-UPDRS I, II, III Off, III On, SCOPA-AUT, MoCA, RBDSQ) and imaging markers (Put. Ipsi, Put. Contra, Caud. Ipsi, and Caud. Contra) with all selected PD patients from the PPMI dataset;
- A clinical course map using clinical markers with all selected PD patients from PPMI, ICEBERG and DIGPD datasets: MDS-UPDRS I, II, III Off, III On, SCOPA-AUT and MoCA and MMSE.

For each model, population and individual parameters were estimated. Patients with iRBD were then positioned on these course maps by estimated the individual parameters that best fit the model to the data of each patient. These parameters were compared to that of PD patients.

We performed a sensitivity analysis by estimating three additional models with all selected PD patients from the pooled PPMI, ICEBERG and DIGPD datasets:

- A motor course map using the subparts of MDS-UPDRS III Off: Axial, Bradykinesia, Rigidity, Tremor;
- A cognitive course map using MoCA and MMSE;
- A dysautonomia course map using SCOPA-AUT only.

Average trajectory description with pathological thresholds

To describe in which order the markers became pathological, we computed a threshold above which a value was considered pathological and reported the PA at which this threshold was reached. We used a balanced logistic regression for each marker of interest to estimate the

threshold that best separated the baseline data from control and PD groups, namely the cut-off at which the regression predicts control or PD labels with equal probability (31,32). This procedure is illustrated in Supplementary Fig. 3. To compute these thresholds in the Clinical Course Map, we used all data available from PD patients from all 3 cohorts and healthy controls from PPMI and ICEBERG. There are no healthy controls in DIGPD. For the Multimodal Course Map, we used data from PPMI only. As MDS-UPDRS III On is not available for healthy patients, we do not use any threshold for this variable. For the Clinical Course Map, since MMSE is not available in PPMI we computed the threshold as the MMSE value for which the percentile was equal to that of the pathological threshold computed on MoCA.

Confidence intervals, goodness-of-fit and prediction errors

We estimated the variability of the progression model (population parameters), by calculating confidence intervals from 10 repetitions of a five-fold cross-validation method. We also calculated the goodness-of-fit for the training and prediction errors for the test sets at each resampling iteration.

Analysis of interindividual variability

To investigate differences in disease progression between PDRBD+ and PDRBD- patients, we performed a multivariate linear regression analysis between each individual parameter and the following covariates: age at baseline, sex, RBD label and cohort. As the acceleration factor follows a log-normal distribution, we regressed the log-acceleration factor. We used the Bonferroni method to correct for multiple comparisons (one test for each individual parameter). The *P*-values are shown after correction and the significance level was set to 5% after correction.

Data availability

PPMI data may be accessed as described at https://www.ppmi-info.org/. The DIGPD and ICEBERG data are available from the authors upon reasonable request. Data were analyzed with Leaspy open-source Python software, freely accessible from https://gitlab.com/icm-institute/aramislab/leaspy/.

Results

Participants

Study participants

Data from 1007 patients (919 PD, 88 iRBD) were included into our analysis corresponding to a total of 9060 visits, after excluding patients with only one visit and PD patients with discordant diagnosis of RBD (see Supplementary Fig. 4). Participant characteristics are presented in Table 1 (participant characteristics for each cohort are detailed in Supplementary Table 1). The average follow-up duration (± SD) is 6.2±2.1 years for all PD patients of interest of the PPMI study, 3.1±1.2 years for those of ICEBERG, and 4.8±1.8 years for those of DIGPD. Among the 919 PD patients, 534 (58%) were considered PDRBD+, ranging from 42% (ICEBERG) to 66% (PPMI) in the cohorts. At baseline compared to PDRBD-, PDRBD+ had significantly higher scores for MDS-UPDRS I, II and SCOPA-AUT in all three cohorts ($p<0.005$), and no difference in MDS-UPDRS III and cognitive (MMSE, MOCA) scores (except for MDS UPDRS III on in DIGPD). Patients with iRBD were significantly older and had lower MOCA scores than PD patients and controls. Baseline data from 264 healthy controls were used only to estimate pathological thresholds (68 from ICEBERG, 196 from PPMI). Among the 88 iRBD patients, 16 converted to PD.

PD progression model

The multimodal course map was derived from the 423 PD patients from PPMI and described the typical scenario of PD progression (Fig. 1). Errors in the goodness-of-fit test of the model ranged from 5% to 7%, except for RBDSQ, for which the error was 13% (Supplementary Table 2). We showed, by cross-validation, that the error was no greater when the model was fitted to a new patient than when it was fitted to a patient from the training sample. Therefore, one could analyze the parameters of PD Course Maps estimated on the whole data set.

The estimated age (PA) at which marker values became pathological are shown in Supplementary Table 4 with corresponding thresholds values in Supplementary Table 3. Ninety five percent of patients visits had a PA between 55.3 and 75.3 years, meaning that our model represents about 14 years of the disease course, with a mean diagnosis at 61.2 ± 0.3 PA years. The first alterations observed began with a decrease of SBR in the contralateral putamen 12.8 ± 0.7 years before diagnosis, followed by the contralateral caudate at 7.0 ± 0.4 years. Motor impairments respectively measured with the MDS-UPDRS III off and MDS-UPDRS II became pathological 8.8 ± 0.5 and 4.6 ± 0.7 years before diagnosis respectively. Non-motor impairments occurred later: SCOPA-AUT 2.1 ± 0.3 years, MDRS-UPDRS I 1.4 ± 0.2 years, and RBDSQ 0.5 ± 1.0 years before diagnosis. Cognitive marker (MOCA) was the last to reach our pathological threshold, just after diagnosis.

This scenario was confirmed by the clinical PD course map obtained from the whole dataset pooling the three cohorts (919 PD patients), which showed the same ordering and similar timings of onset (PA) for diagnosis and clinical markers (Supplementary Fig. 5 and Supplementary Table 5).

Individual trajectory variability

The PD course map represents an average of the typical progression, but also estimates individual parameters for each marker and measure the deviation of each patient trajectory from the average progression (see Supplementary Fig. 1 and Supplementary Table 6). In the multimodal course map, the time-shift variance was 9.5 years, indicating approximately a 10-year variability in the age of markers onset between patients. PD patients progressed between 0.58 times (first decile of acceleration factor) slower and 2.19 times faster (last decile) than the mean progression, thus a 4 times difference of the speed of progression between slow and fast progressors.

The standard deviation of the intermarker spacings indicates how variable the onset of a specific marker is over time all other things (pace of progression and age at onset) being equal. Intermarker spacings with the greatest variability were RBDSQ and MoCA (standard deviation of 10.2 and 10.6 years, respectively), followed by SCOPA-AUT (6.8 years), MDS-UPDRS III on (6.7 years), MDS-UPDRS I (5.3 years), and lastly MDS-UPDRS II, MDS-UPDRS III off and imaging (between 2.4 and 4.4 years, Supplementary Table 6).

The analysis of the correlations of the intermarker spacings shows that an earlier or later progression of MDS-UPDRS III Off and On is not associated to that of non-motor clinical markers (RBDSQ, SCOPA-AUT, MDS-UPDRS I, MoCA) (see Supplementary Fig. 2).

Comparison of PD patients with and without RBD

We compared the individual parameters of PD Course Maps between PDRBD+ and PDRBD-. In the multimodal course map, disease onset (overall time-shift) occurred about 2.8 PA years earlier in PDRBD+ than in PDRBD- patients (CI=[-3.6, -2.1], $p<0.01$, Table 2). Intermarker

spacings for MDS-UPDRS I (-1.4 years, CI=[-2.1, -0.7], $p<0.01$) and SCOPA-AUT (-2.8 years, CI=[-3.8, -1.8], $p<0.01$) indicated an earlier onset in PDRBD+ patients, whereas intermarker spacings for MDS-UPDRS III indicated a later onset in both the off (1.6 years, CI=[1.0, 2.2] $p<0.001$) and on (1.9 years, CI=[1.2, 2.6], $p<0.001$) states. There was no significant difference in the overall speed of progression. Analyses of the clinical course map yielded similar results as in the multimodal course map (Supplementary Table 7).

However, the sensitivity analysis showed that PDRBD+ patients had a significantly faster speed of progression in the cognitive course map (1.38 times faster, log-acceleration factor of 0.32 CI=[0.15, 0.41], p<0.01, Supplementary Table 8) but not in the motor and dysautonomia course maps. In this analysis, PDRBD+ also had a significantly earlier time-shift in the dysautonomia course map (-4.8 years, CI=[-5.9, -3.7], p<0.01) and cognitive course map (-0.37 years, CI=[-0.62, -0.12], p=0.015), but not in the motor course map (Supplementary Table 8).

In the clinical course map, we used the mean values of the individual parameters in each group to calculate the corresponding typical progression scenarios, combining the differences in time-shift, acceleration factor and intermarker spacings (Fig. 2A). The PA at which marker values became pathological for PDRBD- and PDRBD+ are shown in Supplementary Table 4. Compared to PDRBD-, PDRBD+ had a similar onset of motor symptoms (the overall earlier disease onset compensating the later motor changes onset). PDRBD- patients did not reach pathological threshold for any of the non-motor markers at diagnosis, whereas PDRBD+ showed significant changes in SCOPA-AUT, MDRS UPDRS I before diagnosis, and in MOCA and MMSE at diagnosis.

Progression in isolated RBD as compared to PD patients

The specific disease course of iRBD patients is shown in Fig. 2B (PA at which markers became pathological are given in Supplementary Table 4). Mean PA at diagnosis was 74.3 ± 0.1 years, 14 years older than the mean age at onset in PD patients. Following sleep disorders (RBDSQ), the disease course appeared to start with autonomic dysfunction (SCOPA-AUT, 63.6 ± 0.3 years), then cognitive impairment (MOCA, 65.7 ± 0.4 years), deterioration of non-motor daily living activities (MDS UPDRS I, 66.6 ± 0.1 years), and lastly motor abnormalities (70.2 ± 0.3 years for MDS-UPDRS II and 69.12 ± 0.2 years for the MDS-UPDRS III off).

Fig. 3 shows the distributions of the parameters of iRBD patients overlaid with the distributions from PDRBD+ and PDRBD- patients. The speed of progression was similar between the three groups, but the time-shift was earlier in PDRBD+ than in PDRBD- patients, and much later in iRBD patients (Fig. 3A). As expected, intermarker spacing in iRBD differed from both groups of PD patients, earlier for RBDSQ and later for MDS UPDRS III (Fig. 3B). Patients with iRBDs also had earlier MDS UPDRS I and MOCA impairment as compared to the two other groups (Fig. 3C-D).

Discussion

In this study, we modeled the progression of PD in its different dimensions (motor, non-motor, imaging) and components (time shift, speed of progression, sequence of markers), from the prodromal to the symptomatic stage. On average the first changes occurred in the contralateral putamen 13 years before diagnosis with an important heterogeneity of progression patterns within the PD population. Patients with RBD had earlier non-motor symptoms and more rapid progression of dysautonomia and cognitive decline than PD patients without RBD. PD patients

with RDB presented an intermediate progression pattern between that of patients with iRBD and with PD without RBD.

The mean 13-year duration to PD diagnosis of dopamine transporter changes in the contralateral putamen is consistent with previous results from dopaminergic radiotracer imaging (33–39) and with compensatory mechanisms maintaining normal motor function during the early stages of degeneration (40). Our model proposes a typical sequence of symptoms starting with motor symptoms, followed by dysautonomia, sleep disorders starting before diagnosis, and finally cognitive impairment. Motor symptoms onset was estimated on average 9 years before diagnosis in our model confirming that mild motor symptoms occur several years before conversion (41). It should be noted that the "pathological threshold" defined here by a normalization of the scores across the population was not a "clinically significant" threshold that would have led to a diagnosis of PD.

Our model also highlighted the important heterogeneity of individual trajectories showing a variation of more than 10 years in the time-shift, a 4-fold difference in speed of progression between slow- and fast-progressing subjects and a large variability within and between markers spacing. Results clearly confirm that there are multiple progression profiles in sporadic PD. PDRBD+ patients had earlier disease onset and changes in clinical scores occurring 3 to 5 years (MDS-UPDRS II, MoCA, MDS-UPDRS I), 7 years (SCOPA-AUT) and 16 years (RDBSQ) earlier than in PDRBD- patients. PDRBD+ patients had an earlier onset of most non-motor signs that often occurred before diagnosis in contrast to PDRBD- patients who experienced a longer period with only motor symptoms before diagnosis (11). Analysis of the cognitive course map showed that cognitive endpoints progressed significantly faster in PDRBD+. By contrast, motor changes were similar in both groups. However, a finer analysis taking into account the duration between onset of RBD and PD diagnosis showed that a sooner occurrence

of RBD was associated with a higher acceleration factor in the clinical course map (as well as a sooner MDS-UPDRS I onset and later dopamine transporter changes in caudate in the multimodal course map), pointing out the need to take into account the timing of RBD onset (Supplementary Table 10). These results further clarify the previous studies which report a faster progression for PD patients with RBD overall (42–48). Imaging studies have also reported different trajectories of the pathological process in the brain of PD with and without RBD (22,23,49). By better quantizing the heterogeneity in disease progression, our model may be used in the future to forecast the progression of endpoints of participants at entry of trial and identify the ones who are the most likely to experience a fast worsening of the outcome without the intervention. This strategy has been shown to increase the statistical power of trials (50).

In isolated RBD, sleep symptoms occurred first, followed by autonomic dysfunction (10.7 years before PD diagnosis), changes in cognition (8.6 years) and non-motor activities of daily living (7.7 years), with motor signs occurring last (5.2 years). Previous studies using different methods reported the same ordering of events with similar time scale (40,41). Interestingly, PDRBD+ patients had a profile intermediate between those of PDRBD- and iRBD patients, mixing characteristics of the two phenotypes.

Disease course mapping applies multivariate analysis to disease modelling (18,19) allowing to uniquely identifying variations due to differences in progression dynamics (e.g. age at onset and speed of progression) and in disease presentation (e.g. relative timing for biomarkers). This method overcomes some of the limitations of previous modeling strategies (17,20,21,27). The temporal alignment of patient data is estimated from the data, not using age at phenoconversion or symptom onset which depend on clinical practice or patient recall. This approach is therefore suitable for application to iRBD patients who have not undergone phenoconversion. It accounts for differences in age at onset and speed of progression. Previous methods clustered patients at

baseline and analyzed the progression of each group *a posteriori* (13), based on longitudinal data (41), subtyped with specific neural network architecture using a generic hidden Markov model framework (51,52) or more specialized methods (53). An event-based model was proposed to build a normative progression scenario for PD patients at risk of developing dementia, trained on cross-sectional data (15). Our method complements event-based or Markov models with estimates of the duration between two events in the patient's life.

The reported Parkinsonian Age at which some biomarkers become abnormal falls in a region where the model is not informed by data. 4 biomarkers out of 11 in the Figure 1 fall outside the region where 95% of the data lie. These PA result from the extrapolation of the logistic progression curves back in time. We extrapolated for a period smaller than 3 years for all biomarkers but the SBR in contralateral putamen that shows already very high levels at inclusion in the studies. More generally, the other PA, like all the results presented here, depend on the model assumptions, as for any modeling work. The analysis of the goodness-of-fit shows that the model assumptions are legitimate to explain the changes observed in the data. The confidence intervals around the logistic curves show the robustness of the estimated curves with respect to changes in the training population. Small changes in the observed data are therefore not likely to make great changes in the regions where the model extrapolates.

Another limitation of this study is the selection of the main PD markers. We selected global scales such as SCOPA-AUT or MDS-UPDRS which can be used as endpoints in clinical trials. Another choice would be to use domain-specific sub-scores assessing pain, anxiety, olfaction, or sleepiness for instance. Such a choice would require the use of modeling techniques combining categorical and ordinal data. Including other clinical, digital, biological and brain imaging markers would be also of interest. RBD was defined clinically, whereas VPG is the gold standard. However, the risk of false RBD diagnosis is rare in PD patients interviewed by

experienced neurologists (54). The PD course map was estimated with data from patients observed after diagnosis. The information for the prediagnostic period was therefore derived by extrapolation of the model. Latest changes in the MDS-UPDRS in iRBD patients also come from an extrapolation of the model in time since most of them were not observed until phenoconversion, reflecting the fact that most iRBD patients followed for a short period of time do not develop motor symptoms. Furthermore, they might develop other synucleinopathies rarer than PD, which increases the group heterogeneity. Future studies should focus on following more iRBD patients over longer periods of time. The progression of the clinical markers was successfully replicated using PPMI only (multimodal map) or the three datasets combined (clinical map). However, imaging data were only available in PPMI. Imaging findings would need to be replicated in other longitudinal datasets including the same imaging and clinical biomarkers. Lastly, the present work does not compare PD trajectory to that of healthy aging. Rather, it focused on building numerical models of natural PD progression and comparing the trajectories of different subgroups of PD patients: PD with RBD, PD without RBD and iRBD. In future works, including longitudinal data from healthy controls would allow to distinguish the estimated early PD trajectories from those of healthy aging, and thus identify biomarkers to track the course of the disease as early as possible.

Conclusion

Using a new statistical model, we analyzed the heterogeneity in PD progression. The presence of RBD during PD progression was associated with earlier dysautonomia and impairments of non-motor aspects of daily living and later onset of motor symptoms. iRBD was a more pronounced form of this progression, with the preservation of motor capacities for a longer period, but earlier cognitive impairment. Our model may be suitable for future stratification of

PD patients, an important issue to move toward personalized medicine in PD and other neurodegenerative diseases.

Patient consent

Patients gave informed consent for the use of their data in this research. The PPMI, ICEBERG and DIG-PD protocols were approved by the ethics committees of the institutions at which the studies were conducted.

Acknowledgements

We are very grateful to the participants of the PPMI, DIG-PD and ICEBERG studies, on whose data this analysis was based.

Editorial support, in the form of medical writing and copyediting, was provided by Julie Sappa of Alex Edelman and Associates. CdF, RC conducted the research, IA, GM, SLS, PD analysed data, MV, JCC, SL, SD designed and supervised the research, all authors contribute to the writing of the paper.

The DIGPD Study Group members include: Jean-Christophe Corvol, Alexis Elbaz, Marie Vidailhet, Alexis Brice, Fanny Artaud, Frédéric Bourdain, Jean-Philippe Brandel, Pascal Derkinderen, Franck Durif, Richard Levy, Fernando Pico, Olivier Rascol, Anne-Marie Bonnet, Cecilia Bonnet, Christine Brefel-Courbon, Florence Cormier-Dequaire, Bertrand Degos, Bérangère Debilly, Monique Galitsky, David Grabli, Andreas Hartmann, Stephan

Klebe, Julia Kraemmer, Lucette Lacomblez, Sara Leder, Graziella Mangone, Louise-Laure Mariani, Ana-Raquel Marques, Valérie Mesnage, Julia Muellner, Fabienne Ory-Magne, Violaine Planté-Bordeneuve, Emmanuel Roze, Melissa Tir, Hana You, Eve Benchetrit, Julie Socha, Fanny Pineau, Tiphaine Vidal, Elsa Pomies, Virginie Bayet, Suzanne Lesage, Khadija Tahiri, Hélène Bertrand, Alain Mallet, Coralie Villeret, Merry Mazmanian, Hakima Manseur, Mostafa Hajji, Benjamin Le Toullec, Vanessa Brochard, Monica Roy, Isabelle Rieu, Stéphane Bernard, Antoine Faurie-Grepon.

The Iceberg Study Group members include: Marie Vidailhet, Stéphane Lehéricy, Isabelle Arnulf, Jean-Christophe Corvol, Graziella Mangone, , Alexis Elbaz, Richard Levy, David Grabli, Emmanuel Roze, Florence Cormier-Dequaire, Bertrand Degos, Elodie Hainque, Cécile Delorme, Andreas Hartmann, Aurelie Meneret, Louise-Laure Mariani, Clement Tarrano, Cecilia Bonnet, Fernando Pico, Jean-Philippe Brandel, Lucette Lacomblez, Sara Leder, Sara Lambin, Valérie Mesnage, Hana You, Eve Benchetrit, Julie Socha, Fanny Pineau, Marie Alexandrine Glachant, Alize Chalancon, Tiphaine Vidal, Elsa Pomies, Virginie Bayet, Alexis Brice, Suzanne Lesage, Khadija Tahiri, Hélène Bertrand, Alain Mallet, Coralie Villeret, Merry Mazmanian, Hakima Manseur, Mostafa Hajji, Benjamin Le Toullec, Vanessa Brochard, Monica Roy, Isabelle Rieu, Stéphane Bernard, Antoine Faurie-Grepon.

The data used in the preparation of this article were obtained from the Parkinson's Progression Markers Initiative (PPMI) database (https://www.ppmi-info.org/access- data-specimens/download-data). For up-to-date information about this study, visit www.ppmi-info.org. PPMI – a public-private partnership – is funded by The Michael J. Fox Foundation for Parkinson's Research and funding partners, including [list of the full names of all of the

PPMI funding partners can be found at https://www.ppmi-info.org/about-ppmi/who-we-are/study- sponsors].

Supplementary material

Supplementary material is available in the appendix.

References

1. Braak H, Tredici KD, Rüb U, de Vos RAI, Jansen Steur ENH, Braak E. Staging of brain pathology related to sporadic Parkinson's disease. Neurobiol Aging. 2003 Mar 1;24(2):197–211.
2. Berg D, Postuma RB, Adler CH, Bloem BR, Chan P, Dubois B, et al. MDS research criteria for prodromal Parkinson's disease. Mov Disord Off J Mov Disord Soc. 2015 Oct;30(12):1600–11.
3. Halliday G, Hely M, Reid W, Morris J. The progression of pathology in longitudinally followed patients with Parkinson's disease. Acta Neuropathol (Berl). 2008 Apr;115(4):409–15.
4. Halliday GM, McCann H. The progression of pathology in Parkinson's disease. Ann N Y Acad Sci. 2010 Jan;1184:188–95.
5. Greenland JC, Williams-Gray CH, Barker RA. The clinical heterogeneity of Parkinson's disease and its therapeutic implications. Eur J Neurosci. 2019 Feb;49(3):328–38.
6. Venuto CS, Potter NB, Dorsey ER, Kieburtz K. A review of disease progression models of Parkinson's disease and applications in clinical trials. Mov Disord Off J Mov Disord Soc. 2016 Jul;31(7):947–56.
7. Cilia R, Cereda E, Akpalu A, Sarfo FS, Cham M, Laryea R, et al. Natural history of motor symptoms in Parkinson's disease and the long-duration response to levodopa. Brain J Neurol. 2020 Aug 1;143(8):2490–501.
8. Aleksovski D, Miljkovic D, Bravi D, Antonini A. Disease progression in Parkinson subtypes: the PPMI dataset. Neurol Sci Off J Ital Neurol Soc Ital Soc Clin Neurophysiol. 2018 Nov;39(11):1971–6.
9. Lawton M, Ben-Shlomo Y, May MT, Baig F, Barber TR, Klein JC, et al. Developing and validating Parkinson's disease subtypes and their motor and cognitive progression. J Neurol Neurosurg Psychiatry. 2018 Dec;89(12):1279–87.
10. De Pablo-Fernández E, Lees AJ, Holton JL, Warner TT. Prognosis and Neuropathologic Correlation of Clinical Subtypes of Parkinson Disease. JAMA Neurol. 2019 Apr 1;76(4):470–9.
11. Fereshtehnejad SM, Romenets SR, Anang JBM, Latreille V, Gagnon JF, Postuma RB. New Clinical Subtypes of Parkinson Disease and Their Longitudinal Progression: A Prospective Cohort Comparison With Other Phenotypes. JAMA Neurol. 2015 Aug 1;72(8):863–73.
12. Duarte Folle A, Paul KC, Bronstein JM, Keener AM, Ritz B. Clinical progression in Parkinson's disease with features of REM sleep behavior disorder: A population-based

longitudinal study. Parkinsonism Relat Disord. 2019 May;62:105–11.
13. Fereshtehnejad SM, Zeighami Y, Dagher A, Postuma RB. Clinical criteria for subtyping Parkinson's disease: biomarkers and longitudinal progression. Brain. 2017 Jul 1;140(7):1959–76.
14. Severson KA, Chahine LM, Smolensky LA, Dhuliawala M, Frasier M, Ng K, et al. Discovery of Parkinson's disease states and disease progression modelling: a longitudinal data study using machine learning. Lancet Digit Health. 2021 Sep;3(9):e555–64.
15. Oxtoby NP, Leyland LA, Aksman LM, Thomas GEC, Bunting EL, Wijeratne PA, et al. Sequence of clinical and neurodegeneration events in Parkinson's disease progression. Brain. 2021 Mar 1;144(3):975–88.
16. Marras C, Chaudhuri KR. Nonmotor features of Parkinson's disease subtypes. Mov Disord. 2016;31(8):1095–102.
17. Iddi S, Li D, Aisen PS, Rafii MS, Litvan I, Thompson WK, et al. Estimating the Evolution of Disease in the Parkinson's Progression Markers Initiative. Neurodegener Dis. 2018;18(4):173–90.
18. Schiratti JB, Allassonniere S, Colliot O, Durrleman S. Learning spatiotemporal trajectories from manifold-valued longitudinal data. In: Advances in Neural Information Processing Systems. 2015. p. 2404–12.
19. Schiratti JB, Allassonnière S, Colliot O, Durrleman S. A Bayesian Mixed-Effects Model to Learn Trajectories of Changes from Repeated Manifold-Valued Observations. J Mach Learn Res. 2017;18(133):1–33.
20. Koval I, Bône A, Louis M, Lartigue T, Bottani S, Marcoux A, et al. AD Course Map charts Alzheimer's disease progression. Sci Rep. 2021 Apr 13;11(1):8020.
21. Koval I, Dighiero-Brecht T, Tobin AJ, Tabrizi SJ, Scahill RI, Tezenas du Montcel S, et al. Forecasting individual progression trajectories in Huntington disease enables more powered clinical trials. Sci Rep. 2022 Nov 7;12(1):18928.
22. Horsager J, Andersen KB, Knudsen K, Skjærbæk C, Fedorova TD, Okkels N, et al. Brain-first versus body-first Parkinson's disease: a multimodal imaging case-control study. Brain. 2020;143(10):3077–88.
23. Pyatigorskaya N, Yahia-Cherif L, Valabregue R, Gaurav R, Gargouri F, Ewenczyk C, et al. Parkinson Disease Propagation Using MRI Biomarkers and Partial Least Squares Path Modeling. Neurology. 2021 Jan 19;96(3):e460–71.
24. Berg D, Borghammer P, Fereshtehnejad SM. Prodromal Parkinson disease subtypes — key to understanding heterogeneity. Nat Rev Neurol Publ Online April. 2021;20.
25. Corvol JC, Artaud F, Cormier-Dequaire F, Rascol O, Durif F, Derkinderen P, et al. Longitudinal analysis of impulse control disorders in Parkinson disease. Neurology. 2018 Jul 17;91(3):e189–201.
26. Stiasny-Kolster K, Mayer G, Schäfer S, Möller JC, Heinzel-Gutenbrunner M, Oertel WH. The REM sleep behavior disorder screening questionnaire--a new diagnostic instrument. Mov Disord Off J Mov Disord Soc. 2007 Dec;22(16):2386–93.
27. Couronne R, Vidailhet M, Corvol JC, Lehericy S, Durrleman S. Learning Disease Progression Models With Longitudinal Data and Missing Values. In: 2019 IEEE 16th International Symposium on Biomedical Imaging (ISBI 2019). 2019. p. 1033–7.
28. Liu Y, Lawton MA, Lo C, Bowring F, Klein JC, Querejeta-Coma A, et al. Longitudinal Changes in Parkinson's Disease Symptoms with and Without RAPID EYE MOVEMENT Sleep Behavior Disorder: The Oxford Discovery Cohort Study. Mov Disord. 2021 Dec;36(12):2821–32.
29. Fereshtehnejad SM, Yao C, Pelletier A, Montplaisir JY, Gagnon JF, Postuma RB. Evolution of prodromal Parkinson's disease and dementia with Lewy bodies: a prospective study. Brain J Neurol. 2019;142(7):2051–67.

30. Darweesh SKL, Verlinden VJA, Stricker BH, Hofman A, Koudstaal PJ, Ikram MA. Trajectories of prediagnostic functioning in Parkinson's disease. Brain. 2017 Feb;140(2):429–41.
31. Jack CR, Wiste HJ, Weigand SD, Therneau TM, Lowe VJ, Knopman DS, et al. Defining imaging biomarker cut points for brain aging and Alzheimer's disease. Alzheimers Dement J Alzheimers Assoc. 2017 Mar;13(3):205–16.
32. Martínez-Martín P, Rodríguez-Blázquez C, Mario Alvarez null, Arakaki T, Arillo VC, Chaná P, et al. Parkinson's disease severity levels and MDS-Unified Parkinson's Disease Rating Scale. Parkinsonism Relat Disord. 2015 Jan;21(1):50–4.
33. Vingerhoets FJ, Snow BJ, Lee CS, Schulzer M, Mak E, Calne DB. Longitudinal fluorodopa positron emission tomographic studies of the evolution of idiopathic parkinsonism. Ann Neurol. 1994 Nov;36(5):759–64.
34. Moeller JR, Eidelberg D. Divergent expression of regional metabolic topographies in Parkinson's disease and normal ageing. Brain J Neurol. 1997 Dec;120 (Pt 12):2197–206.
35. Morrish PK, Rakshi JS, Bailey DL, Sawle GV, Brooks DJ. Measuring the rate of progression and estimating the preclinical period of Parkinson's disease with [18F]dopa PET. J Neurol Neurosurg Psychiatry. 1998 Mar;64(3):314–9.
36. Stoessl AJ. Positron emission tomography in premotor Parkinson's disease. Parkinsonism Relat Disord. 2007;13 Suppl 3:S421-424.
37. Nandhagopal R, Kuramoto L, Schulzer M, Mak E, Cragg J, Lee CS, et al. Longitudinal progression of sporadic Parkinson's disease: a multi-tracer positron emission tomography study. Brain J Neurol. 2009 Nov;132(Pt 11):2970–9.
38. Fuente-Fernández R de la, Schulzer M, Kuramoto L, Cragg J, Ramachandiran N, Au WL, et al. Age-specific progression of nigrostriatal dysfunction in Parkinson's disease. Ann Neurol. 2011;69(5):803–10.
39. Biondetti E, Gaurav R, Yahia-Cherif L, Mangone G, Pyatigorskaya N, Valabrègue R, et al. Spatiotemporal changes in substantia nigra neuromelanin content in Parkinson's disease. Brain J Neurol. 2020 Sep 1;143(9):2757–70.
40. Postuma RB, Lang AE, Gagnon JF, Pelletier A, Montplaisir JY. How does parkinsonism start? Prodromal parkinsonism motor changes in idiopathic REM sleep behaviour disorder. Brain J Neurol. 2012 Jun;135(Pt 6):1860–70.
41. Fereshtehnejad SM, Yao C, Pelletier A, Montplaisir JY, Gagnon JF, Postuma RB. Evolution of prodromal Parkinson's disease and dementia with Lewy bodies: a prospective study. Brain J Neurol. 2019 Jul 1;142(7):2051–67.
42. Gjerstad MD, Boeve B, Wentzel-Larsen T, Aarsland D, Larsen JP. Occurrence and clinical correlates of REM sleep behaviour disorder in patients with Parkinson's disease over time. J Neurol Neurosurg Psychiatry. 2008 Apr;79(4):387–91.
43. Postuma RB, Gagnon JF, Vendette M, Montplaisir JY. Markers of neurodegeneration in idiopathic rapid eye movement sleep behaviour disorder and Parkinson's disease. Brain J Neurol. 2009 Dec;132(Pt 12):3298–307.
44. Goetz CG, Ouyang B, Negron A, Stebbins GT. Hallucinations and sleep disorders in PD: ten-year prospective longitudinal study. Neurology. 2010 Nov 16;75(20):1773–9.
45. Yoritaka A, Ohizumi H, Tanaka S, Hattori N. Parkinson's Disease with and without REM Sleep Behaviour Disorder: Are There Any Clinical Differences? Eur Neurol. 2009;61(3):164–70.
46. Postuma RB, Gagnon JF, Vendette M, Charland K, Montplaisir J. Manifestations of Parkinson disease differ in association with REM sleep behavior disorder. Mov Disord Off J Mov Disord Soc. 2008 Sep 15;23(12):1665–72.
47. Rolinski M, Szewczyk-Krolikowski K, Tomlinson PR, Nithi K, Talbot K, Ben-Shlomo Y, et al. REM sleep behaviour disorder is associated with worse quality of life and

other non-motor features in early Parkinson's disease. J Neurol Neurosurg Psychiatry. 2014 May 1;85(5):560–6.
48. Romenets SR, Gagnon JF, Latreille V, Panniset M, Chouinard S, Montplaisir J, et al. Rapid eye movement sleep behavior disorder and subtypes of Parkinson's disease. Mov Disord. 2012;27(8):996–1003.
49. Knudsen K, Fedorova TD, Hansen AK, Sommerauer M, Otto M, Svendsen KB, et al. In-vivo staging of pathology in REM sleep behaviour disorder: a multimodality imaging case-control study. Lancet Neurol. 2018 Jul;17(7):618–28.
50. Maheux E, Koval I, Ortholand J, Birkenbihl C, Archetti D, Bouteloup V, et al. Forecasting individual progression trajectories in Alzheimer's disease. Nat Commun. 2023 Feb 10;14(1):761.
51. Mestre TA, Eberly S, Tanner C, Grimes D, Lang AE, Oakes D, et al. Reproducibility of data-driven Parkinson's disease subtypes for clinical research. Parkinsonism Relat Disord. 2018 Nov 1;56:102–6.
52. Zhang X, Chou J, Liang J, Xiao C, Zhao Y, Sarva H, et al. Data-Driven Subtyping of Parkinson's Disease Using Longitudinal Clinical Records: A Cohort Study. Sci Rep. 2019 Jan 28;9(1):1–12.
53. Zhou Y, Tagare HD. Bayesian Longitudinal Modeling of Early Stage Parkinson's Disease Using DaTscan Images. In: Chung ACS, Gee JC, Yushkevich PA, Bao S, editors. Information Processing in Medical Imaging. Springer International Publishing; 2019. p. 405–16. (Lecture Notes in Computer Science).
54. Eisensehr I, Lindeiner H v, Jäger M, Noachtar S. REM sleep behavior disorder in sleep-disordered patients with versus without Parkinson's disease: is there a need for polysomnography? J Neurol Sci. 2001 May 1;186(1):7–11.

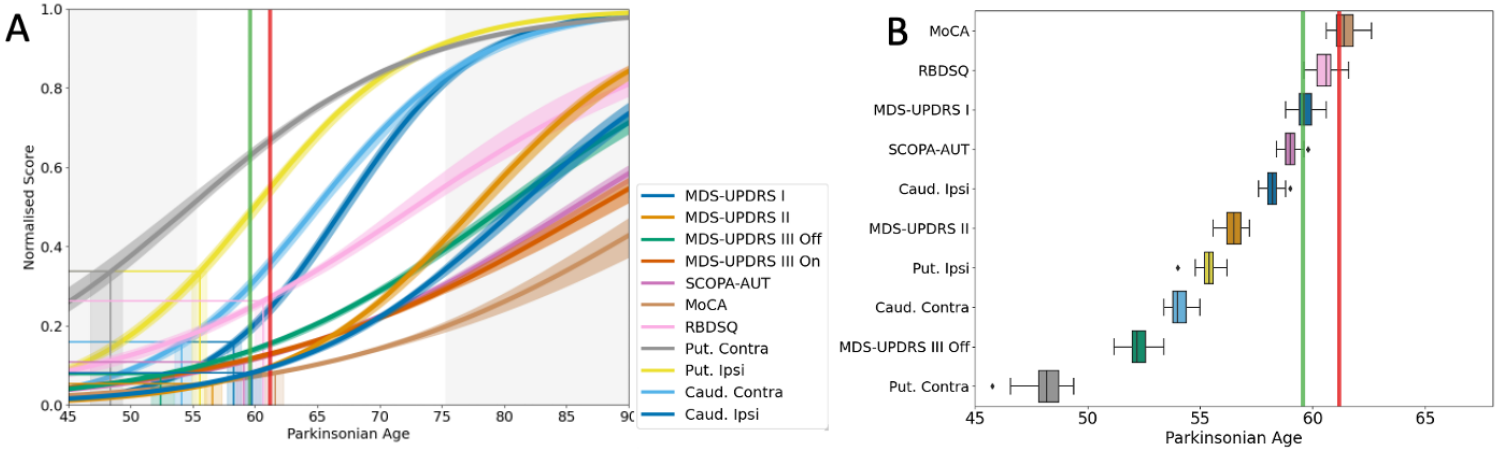

Fig. 1: Typical PD progression of 4 imaging biomarkers and 8 clinical markers in the multimodal course map. A: markers progression* from normal value (0) to maximum pathological change (1) along Parkinsonian Age. Transparent regions show the range of PA where the curves are informed by less than 5% of the data B: timepoints at which markers become abnormal*. Vertical lines indicate PA at first symptoms (green) and PD diagnosis (red). *with 95% confidence intervals.

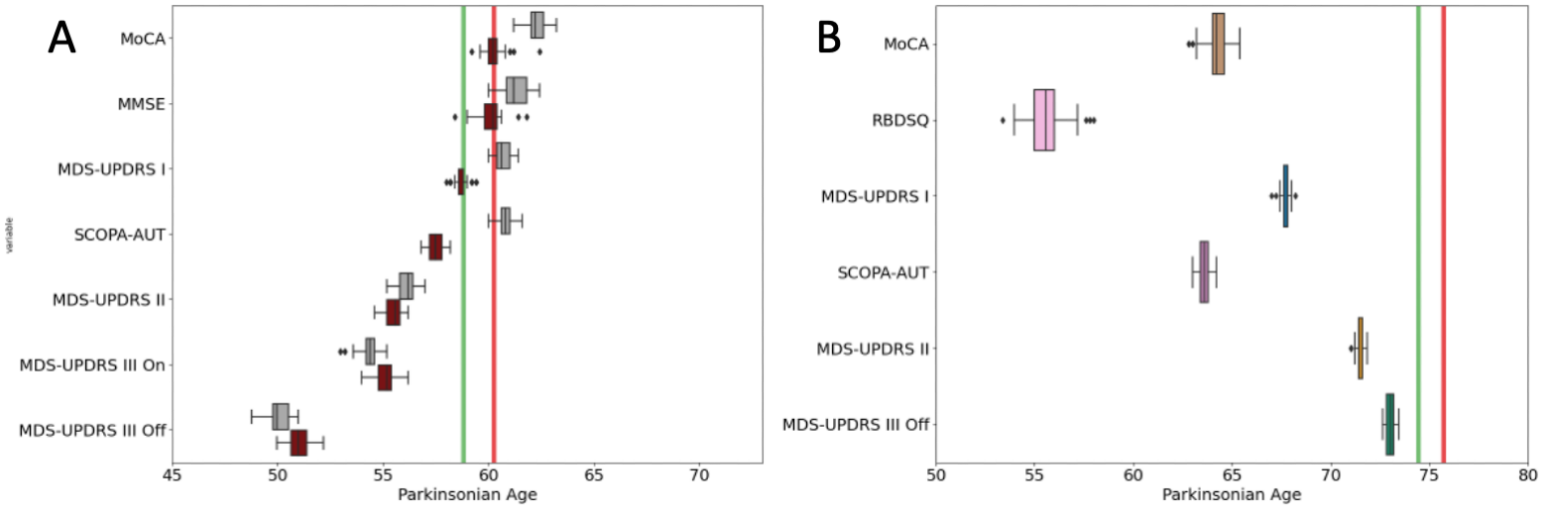

Fig. 2: Typical progression of PDRBD+, PDRBD- and iRBD patients in the clinical course map. The Parkinsonian Age at which clinical markers become pathological for A: PDRBD+ (marron) and PDRBD- (grey), and B: iRBD. Vertical lines indicate the estimated Parkinsonian Age at symptom onset (green) and at PD diagnosis (red).

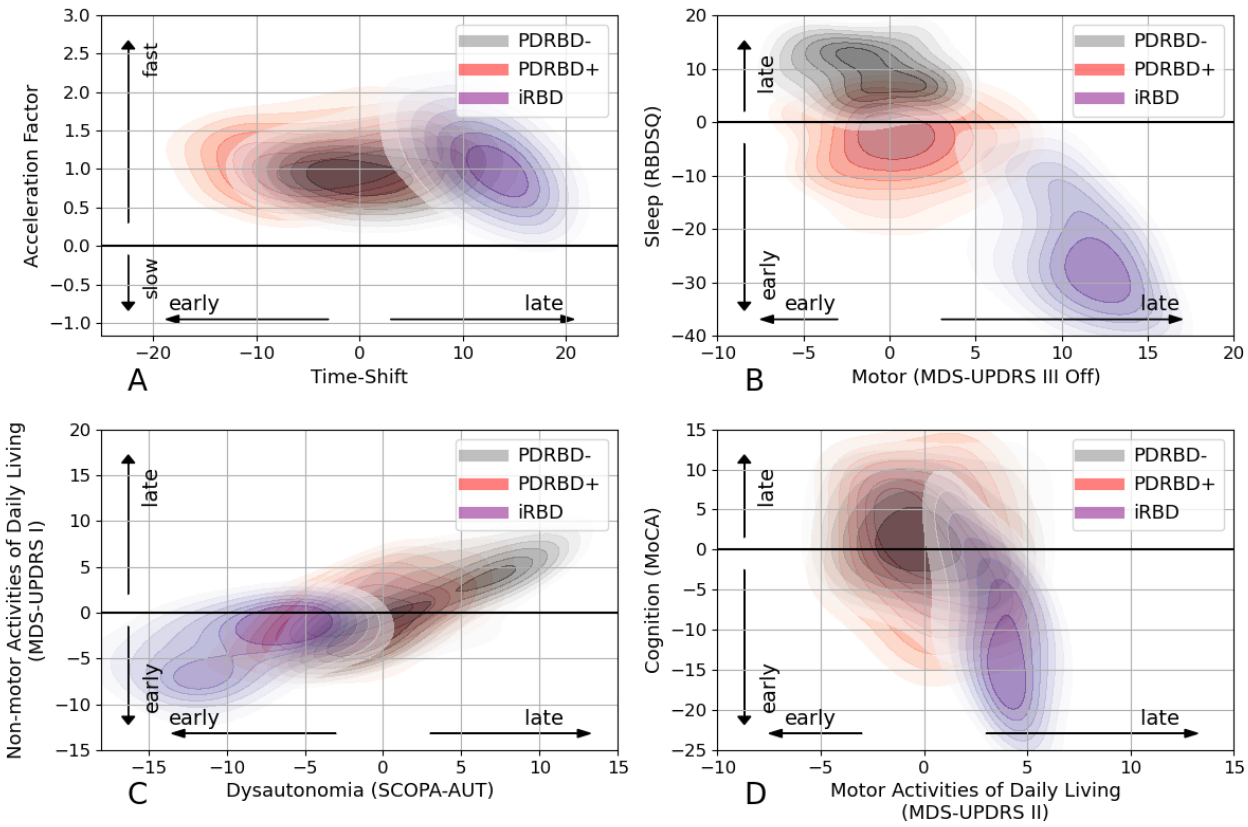

Fig. 3: Distribution of the individual parameters of PDRBD-, PDRBD+ and iRBD patients. Individual parameters are taken from the multimodal course map: acceleration factor versus age at onset (A), followed by pairs of intermarker spacings (B to D).

Table 1: Characteristics of the study participants. For each biomarker, we report mean and standard deviation at baseline. In each column, we report significant differences with respect to the subgroups: controls (a), PDRBD- (b), PDRBD+ (c) or iRBD (d). [1]: disease duration is defined as the difference between baseline age and age at diagnosis. SBR = striatal binding ratio, y = years.

		Control	iRBD	PD		
				Total	PDRBD-	PDRBD+
General information	Total patients	264	88	919	385	534
	Male/female	164/100 (d)	77/11 (c,a,b)	579/340	219/166 (c,d)	360/174 (b,d)
	On PD Medication/Not on PD Medication	1/177 (c,b)	1/87 (c,b)	485/427	229/151 (c,a,d)	256/276 (b,d,a)
	Age (y)	61.0±10.7 (c,d)	68.6±5.6 (c,a,b)	61.8±9.7	61.2±10.2 (c,d)	62.2±9.2 (b,d,a)
	Disease duration (y)[1]	-	-	1.5±1.5	1.6±1.5 (c,d)	1.4±1.4 (b,d)
	Number of visits	7.0±3.2 (c)	7.4±4.9 (c,b)	9.2±5.2	7.8±4.9 (c,d)	10.1±5.2 (b,d,a)
	Study duration (y)	5.1±3.0 (d,b)	3.5±1.6 (c,a,b)	5.2±2.2	4.7±2.2 (c,a,d)	5.6±2.0 (b,d)
	Symptoms duration at diagnosis (y)	-	-	1.2±1.6	1.2±1.6	1.3±1.5
Autonomy & Daily living	MDS-UPDRS I	3.5±3.2 (c,d,b)	8.2±4.7 (c,a,b)	7.1±4.7	6.5±4.4 (c,a,d)	7.6±4.9 (b,d,a)
	SCOPA-AUT	6.1±4.3 (c,d,b)	13.7±7.2 (c,a,b)	10.5±6.7	9.1±6.4 (c,a,d)	11.5±6.8 (b,d,a)
Motor	MDS-UPDRS II	0.6±1.3 (c,d,b)	2.2±2.2 (c,a,b)	6.7±4.4	5.9±4.0 (c,a,d)	7.3±4.5 (b,d,a)
	MDS-UPDRS IIII Off	2.3±3.7 (c,d,b)	8.3±6.0 (c,a,b)	22.8±10.3	22.8±9.4 (a,d)	22.9±10.8 (d,a)
	MDS-UPDRS III On	-	27.9±14.2	22.3±10.7	21.4±10.1	23.0±11.0
	Hoehn&Yahr Off	0.0±0.2 (c,d,b)	0.4±0.8 (c,a,b)	1.7±0.5	1.7±0.5 (c,a,d)	1.6±0.5 (b,d,a)
Cognition	MoCA	28.0±1.4 (c,d,b)	26.3±3.5 (c,a,b)	27.1±2.3	27.2±2.1 (c,a,d)	27.0±2.4 (b,d,a)
	MMSE	29.4±0.9 (c,d,b)	29.0±1.0 (c,a,b)	28.4±1.7	28.6±1.5 (c,a,d)	28.2±1.9 (b,d,a)
Sleep	RBDSQ	2.8±2.3 (c,d,b)	9.0±3.0 (c,a,b)	4.1±2.7	2.4±1.4 (c,a,d)	5.0±2.8 (b,d,a)
Imaging (SBR)	Putamen, contralateral	2.1±0.6 (c,b)	-	0.7±0.3	0.7±0.3 (c,a)	0.7±0.3 (b,a)
	Putamen, ipsilateral	2.1±0.6 (c,b)	-	1.0±0.4	1.0±0.3 (c,a)	0.9±0.4 (b,a)
	Caudate, contralateral	3.0±0.6 (c,b)	-	1.8±0.6	1.9±0.5 (c,a)	1.8±0.6 (b,a)
	Caudate, ipsilateral	3.0±0.6 (c,b)	-	2.2±0.6	2.2±0.6 (c,a)	2.1±0.6 (b,a)

Table 2: Associations between individual parameters in the clinical course map and RBD label with correction for cohort effect, sex and baseline age. Coefficients of regression, 95% confidence intervals and corrected *p*-values are shown. Corrected p-values greater than 1 are set to1. Statistically significant associations are shown in bold typeface.

	Cohort (DIGPD)	Cohort (ICEBERG)	Sex (Female)	Age at Baseline	PDRBD+
Time-shift	**-2.6 (3.4, -1.9), p=1.3e-10**	**-3.4 (-4.5, -2.2), p=1.9e-07**	**1.3 (0.54, 2.0), p=0.0061**	**0.77 (0.74, 0.81), p=2e-211**	**-2.8 (-3.6, -2.1), p=6.8e-13**
Log-Acceleration factor	0.034 (-0.047, 0.12), p=1	**-0.36 (-0.48, -0.23), p=4e-07**	-0.084 (-0.16, -0.0059), p=0.32	**0.011 (0.0069, 0.015), p=7.6e-07**	0.044 (-0.034, 0.12), p=1
MDS-UPDRS I	-0.77 (-1.5, -0.023), p=0.39	**-2.1 (-3.3, -0.95), p=0.0033**	**-2.0 (-2.7, -1.3), p=9.1e-07**	**0.093 (0.057, 0.13), p=4.7e-06**	**-1.4 (-2.1, -0.7), p=0.001**
MDS-UPDRS II	-0.083 (-0.62, 0.46), p=1	-0.029 (-0.86, 0.8), p=1	0.65 (0.12, 1.2), p=0.14	**0.12 (0.095, 0.15), p=6.5e-18**	0.23 (-0.3, 0.75), p=1
MDS-UPDRS III Off	0.13 (-0.49, 0.74), p=1	**-1.3 (-2.2, -0.35), p=0.067**	0.39 (-0.21, 0.99), p=1	**0.052 (0.023, 0.082), p=0.005**	**1.6 (1.0, 2.2), p=6.8e-07**
MDS-UPDRS III On	-0.012 (-0.77, 0.75), p=1	**-1.8 (-3.0, -0.62), p=0.025**	0.73 (-0.0026, 1.5), p=0.46	0.017 (-0.02, 0.054), p=1	**1.9 (1.2, 2.6), p=4.2e-06**
SCOPA-AUT	-0.046 (-1.1, 1.0), p=1	-1.6 (-3.2, -0.004), p=0.45	-0.95 (-2.0, 0.068), p=0.61	**-0.082 (-0.13, -0.031), p=0.014**	**-2.8 (-3.8, -1.8), p=7.2e-07**
MoCA	0.66 (-0.67, 2.0), p=1	**4.4 (2.4, 6.5), p=0.00019**	0.58 (-0.71, 1.9), p=1	**-0.27 (-0.34, -0.21), p=3.5e-15**	-0.23 (-1.5, 1.0), p=1
MMSE	0.57 (-0.4, 1.5), p=1	**3.1 (1.6, 4.6), p=0.00044**	0.47 (-0.47, 1.4), p=1	**-0.17 (-0.21, -0.12), p=6.2e-11**	0.53 (-0.4, 1.5), p=1

		PPMI					ICEBERG					DIGPD		
		Control	iRBD	PD			Control	iRBD	PD			PD		
				Total	PDRBD-	PDRBD+			Total	PDRBD-	PDRBD+	Total	PDRBD-	PDRBD+
General informa-tion	Total patients	196	38	423	145	278	68	50	108	63	45	388	177	211
	Male/female	126/70 (d)	32/6 (a,b)	277/146	82/63 (c,d)	195/83 (b)	38/30 (d)	45/5 (a,b,c)	69/39	37/26 (d)	32/13 (d)	233/155	100/77	133/78
	On PD Medication/Not on PD Medication	1/110	1/37	16/400	7/133	9/267	0/67 (c,b)	0/50 (b,c)	95/13	54/9 (d,a)	41/4 (d,a)	374/14	168/9	206/5
	Age (y)	60.7±11.2 (d)	69.4±5.5 (a,b,c)	61.6±9.7	62.2±9.7 (d)	61.2±9.7 (d)	62.0±9.1 (d)	68.0±5.7 (a,b)	62.0±9.2	59.6±10.0 (d,c)	65.5±6.4 (b)	62.1±9.8	61.0±10.6	62.9±8.9
	Disease duration (y)[1]	-	-	0.6±0.5	0.6±0.6	0.5±0.5	-	-	1.4±1.0	1.3±1.0 (d,c)	1.7±1.0 (d,b)	2.6±1.5	2.6±1.5	2.5±1.5
	Number of visit	8.5±2.2 (b,c,d)	12.7±1.7 (a,c,b)	13.9±3.6	12.9±4.0 (a,c,d)	14.5±3.2 (a,d,b)	2.6±1.3 (d,c,b)	3.4±1.2 (a,c)	3.9±1.0	3.7±1.1 (a)	4.1±1.0 (d,a)	5.4±1.7	5.1±1.7 (c)	5.6±1.6 (b)
	Study duration (y)	6.3±2.4 (b,d)	4.8±0.8 (a,c,b)	6.2±2.1	5.7±2.3 (a,c,d)	6.5±1.9 (d,b)	1.7±1.3 (d,c,b)	2.6±1.3 (a,c)	3.1±1.2	2.9±1.2 (a)	3.3±1.1 (d,a)	4.8±1.8	4.6±1.9 (c)	5.0±1.7 (b)
	Symptoms durations at diagnosis (y)	-	-	1.5±1.9	1.5±2.1	1.4±1.7	-	-	1.7±1.7	1.6±1.7	1.8±1.8	0.9±0.9	0.8±0.9	0.9±1.0
Autonomic & Daily living	MDS-UPDRS I	3.0±3.0 (b,c,d)	7.1±4.0 (a,b)	5.8±4.2	4.8±4.0 (a,c,d)	6.2±4.3 (a,b)	5.0±3.5 (d,c,b)	9.0±5.0 (a,c)	9.7±4.3	8.6±3.9 (a,c)	11.1±4.5 (d,a,b)	7.9±4.8	7.1±4.4 (c)	8.7±5.1 (b)
	SCOPA-AUT	5.8±3.7 (b,c,d)	14.9±8.2 (a,c,b)	9.5±6.1	7.3±4.8 (a,c,d)	10.7±6.5 (a,d,b)	7.2±5.8 (d,c,b)	12.8±6.3 (a,b)	12.5±7.3	10.1±6.3 (d,a,c)	15.7±7.5 (a,b)	11.1±6.9	10.2±7.2 (c)	11.8±6.7 (b)
Motor	MDS-UPDRS II	0.5±1.0 (b,c,d)	2.1±2.4 (a,c,b)	5.7±4.2	4.6±3.4 (a,c,d)	6.3±4.4 (a,d,b)	1.2±1.7 (d,c,b)	2.4±2.1 (a,b,c)	8.0±3.8	6.8±3.7 (d,a,c)	9.7±3.3 (d,a,b)	7.5±4.5	6.7±4.3 (c)	8.2±4.5 (b)
	MDS-UPDRS IIII Off	1.2±2.2 (b,c,d)	4.7±3.9 (a,c,b)	20.4±8.9	19.7±8.1 (a,d)	20.8±9.3 (a,d)	5.6±5.1 (d,c,b)	11.1±6.0 (a,b,c)	29.6±7.5	28.5±7.0 (d,a)	31.2±7.9 (d,a)	28.6±15.8	26.6±14.1	30.2±17.1
	MDS-UPDRS III On	-	25.6±13.9	23.6±11.5	23.7±11.2	23.6±11.6	-	33.3±16.2	26.0±7.6	25.2±7.8	27.1±7.1	20.0±10.1	18.4±9.2 (c)	21.4±10.7 (b)
	Hoehn&Yahr Off	0.0±0.1 (b,c)	0.0±0.0 (c,b)	1.5±0.5	1.5±0.5 (a,d)	1.5±0.5 (a,d)	0.1±0.4 (d,c,b)	0.7±0.9 (a,b,c)	2.0±0.3	2.0±0.2 (d,a,c)	2.1±0.3 (d,a,b)	2.0±0.6	1.9±0.5	2.1±0.6
Cognition	MoCA	28.2±1.1 (b,c,d)	25.5±4.2 (a,c,b)	27.1±2.3	27.3±2.2 (a,d)	27.1±2.4 (a,d)	27.8±2.0	27.3±2.3	27.5±2.0	27.5±1.8	27.6±2.3	-	-	-
	MMSE	-	-	-	-	-	29.4±0.9	29.0±1.0	29.0±1.0	29.0±1.0	29.0±1.1	28.2±1.9	28.4±1.6	28.1±2.0
Sleep	RBDSQ	2.8±2.3 (c,d)	9.0±3.0 (a,c,b)	4.1±2.7	2.4±1.4 (c,d)	5.0±2.8 (a,d,b)	-	-	-	-	-	-	-	-
Imaging (SBR)	Putamen, contralateral	2.1±0.6 (b,c)	-	0.7±0.3	0.7±0.3 (a)	0.7±0.3 (a)	-	-	-	-	-	-	-	-
	Putamen, ipsilateral	2.1±0.6 (b,c)	-	1.0±0.4	1.0±0.3 (a,c)	0.9±0.4 (a,b)	-	-	-	-	-	-	-	-
	Caudate, contralateral	3.0±0.6 (b,c)	-	1.8±0.6	1.9±0.5 (a)	1.8±0.6 (a)	-	-	-	-	-	-	-	-
	Caudate, ipsilateral	3.0±0.6 (b,c)	-	2.2±0.6	2.2±0.6 (a,c)	2.1±0.6 (a,b)	-	-	-	-	-	-	-	-

Supplementary Table 1: Characteristics of the study participants of each cohort. For each biomarker, we report the mean and standard deviation at baseline. In PPMI, drugs were not administered from baseline (which explains the later timing of the first value for MDS-UPDRS III On, 2.0±1.3 years after baseline on average). In each column, we report significant differences with respect to the other subgroups: controls (a), PDRBD- (b), PDRBD+ (c) or iRBD (d). [1]: disease duration is defined as the difference between baseline age and age at diagnosis. Abbreviations: SBR = striatal binding ratio, y = years.

	Multimodal course map		Clinical course map	
	Training	Test	Training	Test
MDS-UPDRS I (0-52 scale)	2.7 ± 0.026	2.7 ± 0.097	2.6 ± 0.024	2.6 ± 0.083
MDS-UPDRS II (0-52 scale)	2.8 ± 0.028	2.8 ± 0.1	2.6 ± 0.025	2.6 ± 0.087
MDS-UPDRS III Off (0-132 scale)	6.3 ± 0.062	6.4 ± 0.21	6.4 ± 0.077	6.4 ± 0.23
MDS-UPDRS III On (0-132 scale)	6.7 ± 0.098	6.7 ± 0.35	6.4 ± 0.081	6.4 ± 0.25
SCOPA-AUT (0-69 scale)	3.5 ± 0.044	3.5 ± 0.16	3.5 ± 0.042	3.5 ± 0.15
MoCA (0-30 scale)	1.7 ± 0.025	1.7 ± 0.093	1.7 ± 0.023	1.7 ± 0.081
MMSE (0-30 scale)			1.5 ± 0.029	1.5 ± 0.096
RBDSQ (0-13 scale)	1.7 ± 0.024	1.7 ± 0.091		
Put. Contra	0.11 ± 0.0023	0.11 ± 0.007		
Put. Ipsi	0.13 ± 0.003	0.14 ± 0.0093		
Caud. Contra	0.2 ± 0.003	0.2 ± 0.0097		
Caud. Ipsi	0.21 ± 0.0036	0.21 ± 0.011		

Supplementary Table 2: Goodness-of-fit and prediction errors. Mean errors for the training and test sets, and standard deviation computed over the 50 resampling folds, for both multimodal and clinical course maps.

	Multimodal course map	Clinical course map
MDS-UPDRS I	4	5
MDS-UPDRS II	3	3
MDS-UPDRS III Off	10	12
SCOPA-AUT	8	9
MoCA	28	28
MMSE	-	29
RBDSQ	3	-
Put. Contra	0.29	-
Put. Ipsi	0.29	-
Caud. Contra	0.53	-
Caud. Ipsi	0.53	-

Supplementary Table 3: Pathological thresholds. Value for each biomarker.

Multimodal course map				
	iRBD	**iPD**	**PDRBD+**	**PDRBD-**
PA at first symptoms	-	59.55±0.27	59.12±0.37	60.2±0.42
PA at diagnosis	-	61.18±0.28	60.73±0.37	61.87±0.41
MDS-UPDRS I	67.8±0.21	59.72±0.38	58.16±0.45	62.77±0.49
MDS-UPDRS II	71.55±0.17	56.54±0.39	55.38±0.51	58.78±0.45
MDS-UPDRS III Off	73.07±0.2	52.36±0.48	52.13±0.55	52.6±0.56
SCOPA-AUT	63.64±0.3	59.04±0.33	56.8±0.41	63.52±0.5
MoCA	64.26±0.6	61.51±0.45	60.28±0.51	63.85±0.59
MMSE	-	-	-	-
RBDSQ	55.71±0.99	60.58±0.39	55.59±0.62	70.91±0.59
Put. Contra	-	48.27±0.68	47.89±0.74	48.87±0.76
Put. Ipsi	-	55.46±0.38	54.81±0.47	56.59±0.48
Caud. Contra	-	54.1±0.37	53.49±0.44	55.17±0.52
Caud. Ipsi	-	58.23±0.29	57.46±0.38	59.64±0.42

Supplementary Table 4: Parkinson age on the multimodal course map at which the typical progression of each biomarker reaches its pathological threshold (and its standard deviation in parentheses). Age is given in years.

Clinical course map				
	iRBD	**PD**	**PDRBD+**	**PDRBD-**
PA at first symptoms	-	58.8±0.22	59.15±0.26	58.18±0.32
PA at diagnosis	-	60.23±0.22	60.61±0.27	59.56±0.32
MDS-UPDRS I	66.61±0.14	59.58±0.29	58.76±0.31	60.73±0.39
MDS-UPDRS II	70.2±0.13	55.82±0.33	55.52±0.36	56.2±0.43
MDS-UPDRS III Off	69.12±0.22	50.73±0.45	51.11±0.49	50.1±0.52
SCOPA-AUT	63.64±0.29	58.88±0.31	57.54±0.33	60.86±0.38
MoCA	65.69±0.41	61.19±0.43	60.37±0.48	62.34±0.48
MMSE	69.18±1.98	60.62±0.56	60.08±0.59	61.34±0.6
RBDSQ	-	-	-	-
Put. Contra	-	-	-	-
Put. Ipsi	-	-	-	-
Caud. Contra	-	-	-	-
Caud. Ipsi		-	-	-

Supplementary Table 5: Parkinson age on the clinical course map at which the typical progression of each biomarker reaches its pathological threshold. Age is given in years.

	Multimodal				Clinical			
	iRBD	**PD**	**PDRBD+**	**PDRBD-**	**iRBD**	**PD**	**PDRBD+**	**PDRBD-**
Acceleration factor first decile	0.7	0.58	0.63	0.55	0.81	0.6	0.61	0.6
Acceleration factor last decile	2.27	2.19	2.25	2.03	3.1	2.79	2.95	2.65
Time-shift std	6.1	9.51	9.47	9.07	6.67	9.31	9.12	9.49
MDS-UPDRS I std	4.99	5.34	5.03	5.8	6.16	5.64	5.63	5.62
MDS-UPDRS II std	2.58	4.17	4.17	4.16	3.61	4.07	4.17	3.92
MDS-UPDRS III Off std	3.91	4.42	4.36	4.15	5.59	4.73	4.67	4.62
MDS-UPDRS III On std	6.55	6.68	6.84	6	6.12	5.32	5.2	5.26
SCOPA-AUT std	6.88	6.81	6.6	6.57	7.8	7.87	7.6	7.96
MoCA std	11.95	10.59	11.03	9.72	11.09	9.51	10.06	8.67
MMSE std					7.07	6.32	6.6	5.92
RBDSQ std	11.23	10.15	8.8	6.4				
Put. Contra std		3.16	3.13	3.06				
Put. Ipsi std		2.39	2.32	2.33				
Caud. Contra std		3.08	3.01	3.06				
Caud. Ipsi std		2.68	2.63	2.63				

Supplementary Table 6: Standard deviation of individual parameters for each group of patients, for both the multimodal and clinical course maps. For the acceleration factor, which follows a log-normal distribution, we show the first and last decile.

	Sex	Age at baseline	PDRBD+
Time-shift	0.59 (CI=[-0.25, 1.4]), p=2.0	0.86 (CI=[0.82, 0.9]), p=2.9e-149	-2.3 (CI=[-3.1, -1.5]), p=1.5e-06
Log-Acceleration factor	-0.078 (CI=[-0.19, 0.031]), p=1.9	0.0065 (CI=[0.0012, 0.012]), p=0.2	0.082 (CI=[-0.027, 0.19]), p=1.7
MDS-UPDRS I	-1.6 (CI=[-2.7, -0.49]), p=0.059	0.0049 (CI=[-0.049, 0.059]), p=10.0	-2.1 (CI=[-3.2, -1.0]), p=0.0026
MDS-UPDRS II	0.85 (CI=[-0.02, 1.7]), p=0.67	0.026 (CI=[-0.016, 0.069]), p=2.7	-0.86 (CI=[-1.7, 0.015]), p=0.65
MDS-UPDRS III Off	0.62 (CI=[-0.26, 1.5]), p=2.0	-0.0061 (CI=[-0.049, 0.037]), p=9.3	1.8 (CI=[0.88, 2.7]), p=0.0012
MDS-UPDRS III On	1.7 (CI=[0.31, 3.0]), p=0.19	-0.09 (CI=[-0.16, -0.024]), p=0.091	2.1 (CI=[0.7, 3.4]), p=0.037
SCOPA-AUT	-0.98 (CI=[-2.4, 0.39]), p=1.9	-0.11 (CI=[-0.18, -0.044]), p=0.014	-4.5 (CI=[-5.8, -3.1]), p=6.4e-09
MoCA	2.7 (CI=[0.6, 4.8]), p=0.14	-0.45 (CI=[-0.55, -0.35]), p=1.4e-15	-0.88 (CI=[-3.0, 1.2]), p=4.9
Put. Contra	-0.72 (CI=[-1.3, -0.12]), p=0.24	0.098 (CI=[0.068, 0.13]), p=2.1e-09	0.8 (CI=[0.2, 1.4]), p=0.11
Put. Ipsi	-0.064 (CI=[-0.53, 0.4]), p=9.5	0.022 (CI=[-0.00085, 0.044]), p=0.71	0.6 (CI=[0.14, 1.1]), p=0.14
Caud. Contra	-0.33 (CI=[-0.93, 0.28]), p=3.5	0.045 (CI=[0.016, 0.075]), p=0.031	0.54 (CI=[-0.069, 1.1]), p=0.99
Caud. Ipsi	0.026 (CI=[-0.51, 0.56]), p=11.0	0.0093 (CI=[-0.017, 0.035]), p=5.8	0.48 (CI=[-0.058, 1.0]), p=0.96

Supplementary Table 7: Association between individual parameters in the multimodal course maps and RBD label, with correction for sex and age at baseline. 95% confidence intervals and corrected *p*-values are shown. Statistically significant associations are shown in bold typeface. Note that, for this experiment, the multimodal course map was retrained without RBDSQ as an endpoint.

	Cohort (DIGPD)	Cohort (ICEBERG)	Sex (Female)	Age at Baseline	PDRBD+
Cognitive Course Map					
Time-shift	-0.17 (-0.42, 0.092), p=0.83	**0.68 (0.28, 1.1), p=0.0033**	**0.46 (0.21, 0.71), p=0.0014**	0.0073 (-0.0051, 0.02), p=1.0	**-0.37 (-0.62, -0.12), p=0.015**
Log-Acceleration factor	**-0.23 (-0.39, -0.13), p=5.7e-04**	0.11 (-0.098, 0.31), p=1.0	0.047 (-0.082, 0.17), p=1.0	**0.018 (0.011, 0.024), p=3.2e-07**	**0.32 (0.15, 0.41), p=7.2e-05**
MoCA	**-6.9 (-9.6, -4.2), p=2.4e-06**	-1.4 (-5.5, 2.8), p=1.0	-2.8 (-5.4, -0.21), p=0.14	0.093 (-0.037, 0.22), p=0.64	-0.77 (-3.4, 1.8), p=1.0
MMSE	**7.6 (4.6, 11.0), p=2.4e-06**	1.5 (-3.0, 6.0), p=1.0	3.1 (0.23, 6.0), p=0.14	-0.1 (-0.24, 0.04), p=0.64	0.85 (-2.0, 3.7), p=1.0
Dysautonomia Course Map					
Time-shift	**-1.7 (-2.9, -0.52), p=0.0094**	**-3.7 (-5.5, -1.8), p=0.00018**	0.3 (-0.85, 1.4), p=1.0	**0.58 (0.52, 0.63), p=3.2e-72**	**-4.8 (-5.9, -3.7), p=1.1e-15**
Log-Acceleration factor	-0.032 (-0.09, 0.024), p=0.52	**-0.093 (-0.19, -0.0096), p=0.06**	**-0.059 (-0.12, -0.0056), p=0.062**	-0.0013 (-0.004, 0.0015), p=0.72	0.056 (-0.00088, 0.11), p=0.11
Motor Course Map					
Time-shift	-3.8 (-8.8, 1.2), p=0.81	**-4.5 (-5.6, -3.4), p=3.2e-14**	**2.1 (1.2, 3.0), p=5.9e-05**	**0.8 (0.76, 0.85), p=2.7e-139**	-0.39 (-1.3, 0.51), p=1.0
Log-Acceleration factor	0.48 (-0.25, 1.0), p=1.0	**-0.19 (-0.36, -0.074), p=0.018**	-0.12 (-0.25, -0.016), p=0.15	0.0037 (-0.0021, 0.0095), p=1.0	0.058 (-0.06, 0.17), p=1.0
MDS-UPDRS III Off - Axial	0.004 (-3.4, 3.4), p=1.0	-0.95 (-1.7, -0.2), p=0.08	0.54 (-0.086, 1.2), p=0.55	**0.1 (0.069, 0.13), p=2.2e-09**	0.24 (-0.38, 0.87), p=1.0
MDS-UPDRS III Off - Bradykinesia	-1.1 (-4.8, 2.5), p=1.0	-0.58 (-1.4, 0.23), p=0.96	**1.3 (0.64, 2.0), p=0.00078**	**-0.054 (-0.087, -0.021), p=0.0086**	0.28 (-0.39, 0.95), p=1.0
MDS-UPDRS III Off - Rigidity	-0.48 (-5.4, 4.4), p=1.0	**2.4 (1.3, 3.5), p=0.00013**	**-1.7 (-2.6, -0.85), p=0.00087**	**-0.13 (-0.18, -0.087), p=6.4e-08**	0.25 (-0.64, 1.1), p=1.0
MDS-UPDRS III Off - Tremor	4.4 (-11.0, 20.0), p=1.0	-1.2 (-4.6, 2.2), p=1.0	-0.56 (-3.4, 2.3), p=1.0	0.049 (-0.091, 0.19), p=1.0	-2.7 (-5.6, 0.094), p=0.35

Supplementary Table 8: Associations between individual parameters in each supplementary course maps and RBD label with correction for cohort effect, sex and baseline age. Coefficients of regression, 95% confidence intervals and corrected *p*-values are shown. Corrected p-values greater than 1 are set to1. Statistically significant associations are shown in bold typeface.

	Clinical Course Map			Multimodal Course Map		
	PDRBD+ with RBD onset before inclusion (Mean ± SD)	PDRBD+ with RBD onset after inclusion (Mean ± SD)	P	PDRBD+ with RBD onset before inclusion (Mean ± SD)	PDRBD+ with RBD onset after inclusion (Mean ± SD)	P
Log-Acceleration Factor	0.33 ± 0.61	0.25 ± 0.63	1.30E-01	0.23 ± 0.55	0.12 ± 0.53	1.17E-01
Time-shift	63.85 ± 9.21	64.52 ± 9.18	3.97E-01	63.56 ± 10.13	64.35 ± 8.92	4.99E-01
MDS-UPDRS I	0.0 ± 0.05	-0.0 ± 0.05	5.16E-01	**0.02 ± 0.07**	**-0.01 ± 0.06**	**7.75E-03**
MDS-UPDRS II	-0.0 ± 0.05	-0.01 ± 0.06	5.32E-01	0.02 ± 0.07	-0.01 ± 0.06	**1.33E-03**
MDS-UPDRS III Off	-0.01 ± 0.05	-0.01 ± 0.05	2.87E-01	-0.01 ± 0.05	-0.01 ± 0.06	5.20E-01
MDS-UPDRS III On	-0.01 ± 0.04	-0.01 ± 0.05	6.83E-01	-0.0 ± 0.06	-0.01 ± 0.06	1.18E-01
SCOPA-Aut	0.01 ± 0.06	0.0 ± 0.06	1.31E-01	**0.03 ± 0.07**	**-0.0 ± 0.06**	**9.42E-05**
MoCA	0.01 ± 0.05	0.01 ± 0.05	5.95E-01	**0.02 ± 0.07**	**-0.0 ± 0.06**	**2.76E-02**
MMSE	0.0 ± 0.02	0.0 ± 0.02	3.04E-01			
PUTAMEN CONTRALATERAL				**-0.02 ± 0.06**	**0.0 ± 0.05**	**7.72E-06**
PUTAMEN IPSILATERAL				**-0.02 ± 0.07**	**0.01 ± 0.05**	**8.47E-04**
CAUDATE CONTRALATERAL				**-0.02 ± 0.1**	**0.02 ± 0.09**	**5.50E-04**
CAUDATE IPSILATERAL				**-0.02 ± 0.11**	**0.02 ± 0.09**	**3.44E-03**

Supplementary Table 9: Individual parameters mean comparison between PDRBD+ patients that were RBD+ from the beginning of the study versus PDRBD+ patients who turned RBD+ during the course of the study. Statistically significant associations are shown in bold typeface. P-values correspond to two-sided t-tests between group means.

	Clinical Course Map		Multimodal Course Map	
	Time between diagnosis and RBD onset	P-value	Time between diagnosis and RBD onset	P-value
Log-Acceleration Factor	**-0.21 ± 0.06**	**4.40E-04**	-0.15 ± 0.08	5.22E-02
Time-shift	-0.04 ± 0.06	5.24E-01	0.02 ± 0.08	8.26E-01
MDS-UPDRS I	-0.03 ± 0.06	6.01E-01	**-0.16 ± 0.08**	**3.42E-02**
MDS-UPDRS II	0.02 ± 0.06	7.85E-01	-0.09 ± 0.08	2.40E-01
MDS-UPDRS III Off	0.06 ± 0.06	3.33E-01	-0.05 ± 0.08	5.04E-01
MDS-UPDRS III On	0.05 ± 0.06	4.06E-01	-0.06 ± 0.08	4.00E-01
SCOPA-Aut	-0.05 ± 0.06	4.29E-01	-0.12 ± 0.08	1.31E-01
MoCA	-0.01 ± 0.06	7.93E-01	-0.13 ± 0.07	8.03E-02
MMSE	-0.0 ± 0.06	9.90E-01		
PUTAMEN CONTRALATERAL			0.13 ± 0.07	8.08E-02
PUTAMEN IPSILATERAL			0.12 ± 0.08	1.09E-01
CAUDATE CONTRALATERAL			**0.16 ± 0.08**	**3.89E-02**
CAUDATE IPSILATERAL			**0.17 ± 0.08**	**3.11E-02**

Supplementary Table 10: Associations between individual parameters and duration between PD diagnosis and RBD onset in PDRBD+ patients with for whom RBD occurred in the course of the study. For each individual parameter, the effect of *Time between diagnosis and RBD onset* is tested in a linear regression accounting for cohort effect (for the Clinical Course Map), sex and baseline age (except when time-shift is the dependent variable, as it strongly correlates with baseline age). The Multimodal Course Map analysis included PDRBD+ patients of the PPMI study, and the Clinical Course Map also included the PDRBD+ patients from DIGPD (PDRBD+ patients with RBD first occurrence in the course of the disease were too few in the ICEBERG cohort: N=11). Standardized coefficients of regression, SE and *p*-values associated to the parameter t-test are shown. Statistically significant associations are shown in bold typeface.

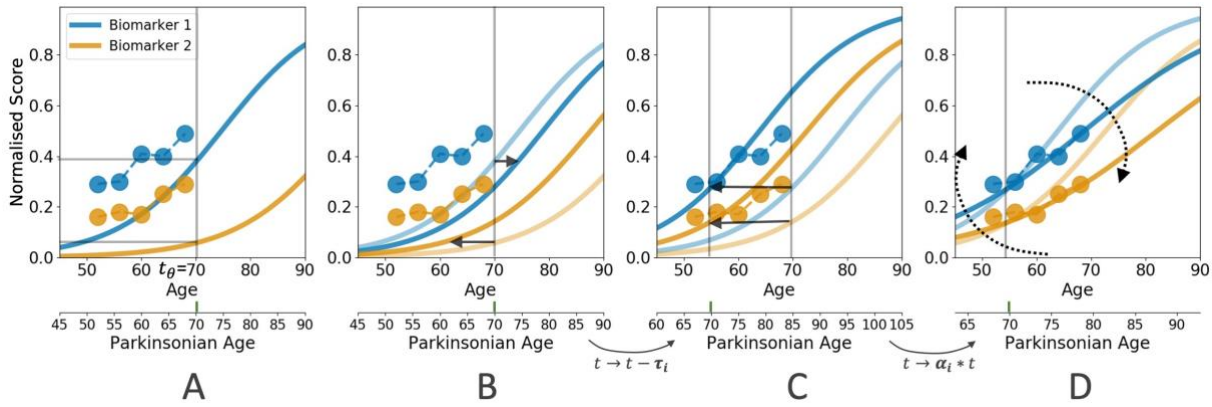

Supplementary Fig. 1: Positioning of a subject on the PD course map. A) The typical progression of two biomarkers (blue and yellow) is shown by plain logistic curves together with the corresponding biomarker values of one subject at five successive visits. Biomarker values are normalised such that 0 corresponds to the normal value and 1 as the maximal pathological change (see Methods). B-to-D) A series of operations is used to transform the model to fit the data for the subject and, therefore, to determine the subject's specific trajectory. The intermarker spacings modify the relative timing between the two curves (B), the time-shift translates all curves by the same amount of time (C) and the acceleration factor stretches the curves (D). Note that here the two intermarker spacing have opposite signs not to interfere with the time-shift (a similar condition holds for more than 2 biomarkers). Time-shift and accelearation factors map the actual age of the patient to the corresponding Parkinsonian age. We estimate the shape and position of the logistic curves, such that the mean time-shift, intermarker spacing, and log-acceleration factor for all subjects in the longitudinal training dataset are zero. Relative to this population trajectory, each subject is characterized by its individual parameters (intermarker spacings, time-shift, acceleration factor). For example, a 1-year intermarker spacing for a marker means that the changes to that marker occur one year later than would typically be the case. A 1-year time-shift means that markers overall reach the same values one year later than in a typical patient. An acceleration factor of 2 means marker changes are achieved in half the time they would be in a typical patient (twice as long for an acceleration factor of 0.5).

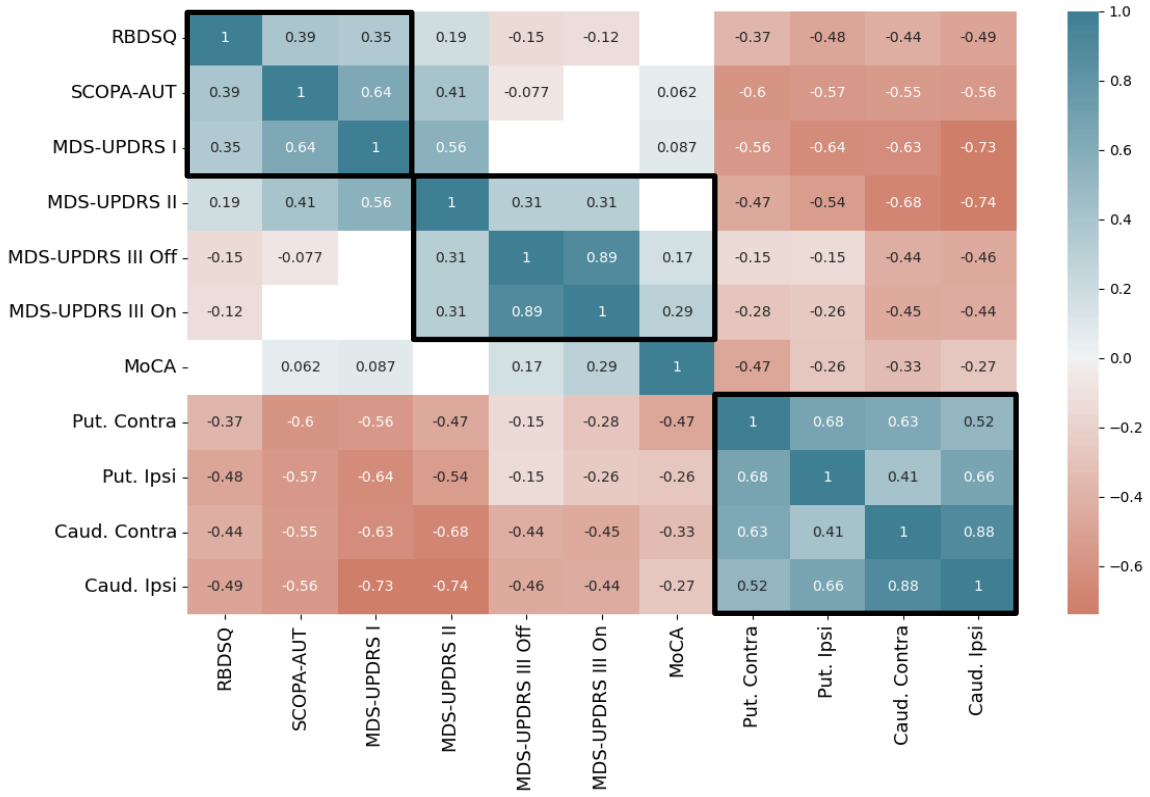

Supplementary Fig. 2: Correlation matrix of intermarker spacings. Teal-colored shading indicates positive correlations. Peach-colored shading indicates negative correlations. Only statistically significant correlation coefficients are shown. After positioning each PD patient on the multimodal course map, we calculated the correlation matrix for intermarker spacing, and we report correlation coefficients significant at the 90% level, showing how the different markers jointly evolve. The correlation matrix of intermarker spacing showed three main clusters of markers (Fig. 3): the group of non-motor clinical markers (RBDSQ, SCOPA-AUT, MDS-UPDRS I), the group of motor clinical markers (MDS-UPDRS III on, MDS-UPDRS III off) and the group of imaging markers (Caud and Put). This implies that if one of the markers in a cluster occurred earlier in the course of the disease, then all the other markers in the cluster also tended to occur earlier. Consistent results were obtained on the clinical course map for non-imaging markers (Supplementary Table 5).

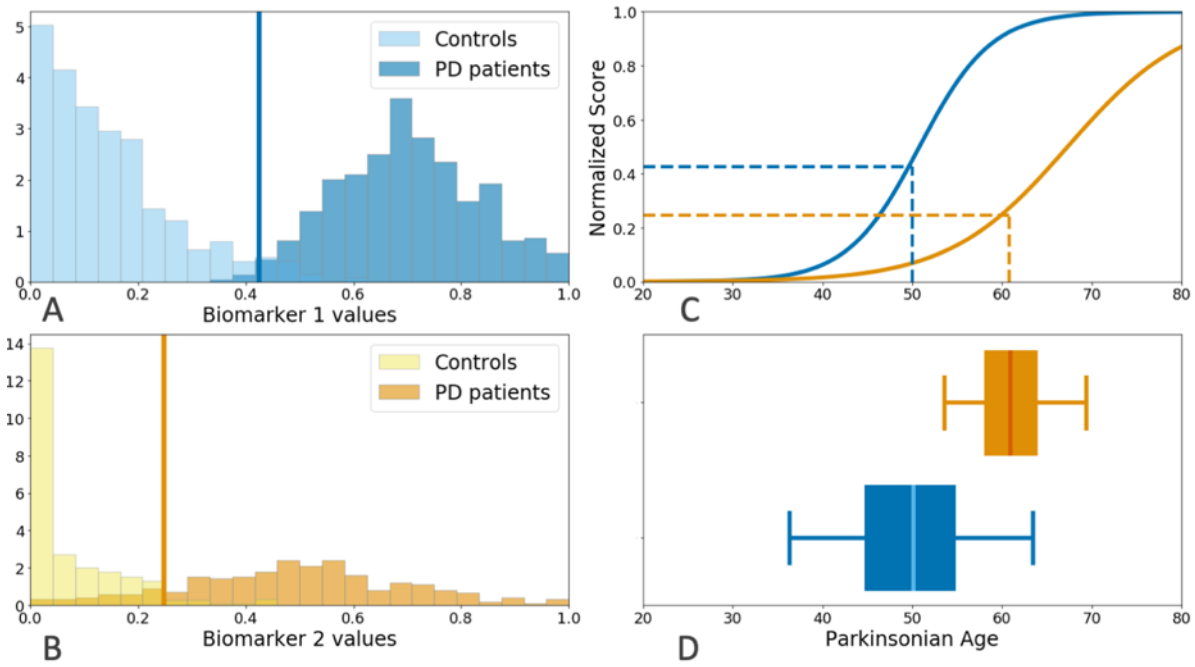

Supplementary Fig. 3: Illustration of pathological thresholds on PD course maps. A logistic regression method was used to determine the thresholds best separating controls from PD patients at baseline for each endpoint (A,B). The thresholds are reported on the *y*-axis of the PD course map. The Parkinsonian age at which the endpoint become pathological is determined (C). We report the series of PAs for each endpoint, together with the confidence interval, on the reference timeline (D).

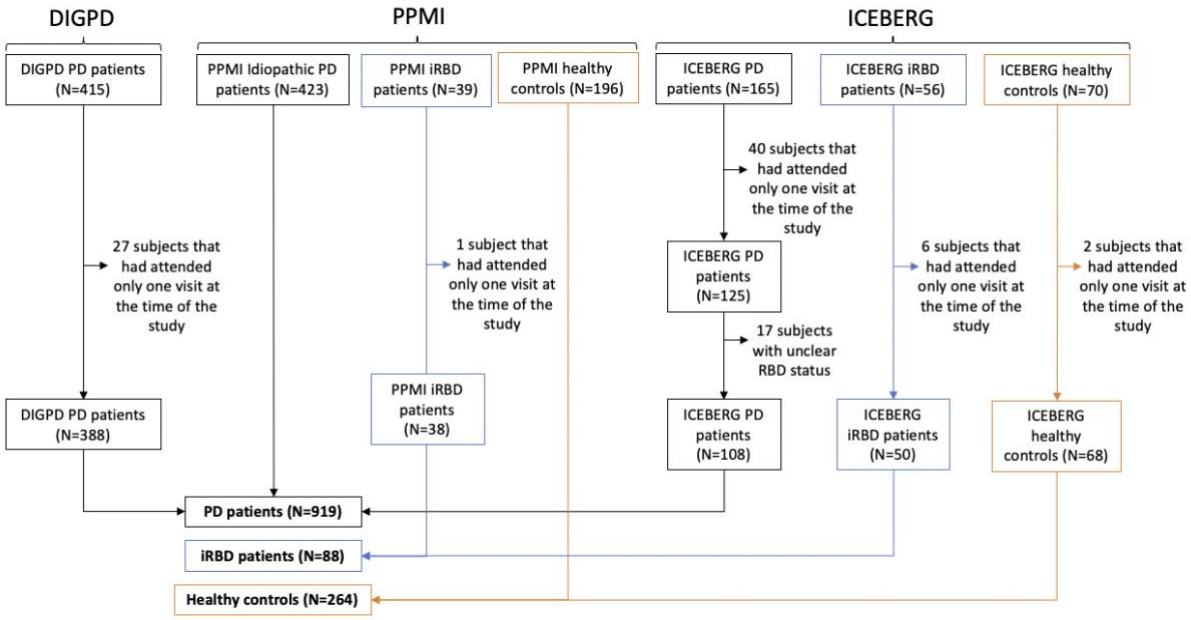

Supplementary Figure 4: Flowchart of the patients selection. PD patients, iRBD patients and healthy controls are included from the PPMI, DIGPD and ICEBERG studies.

*unclear RBD status: status confirmed by video and sleep monitoring but not by the RBDSQ-HK questionnaire.

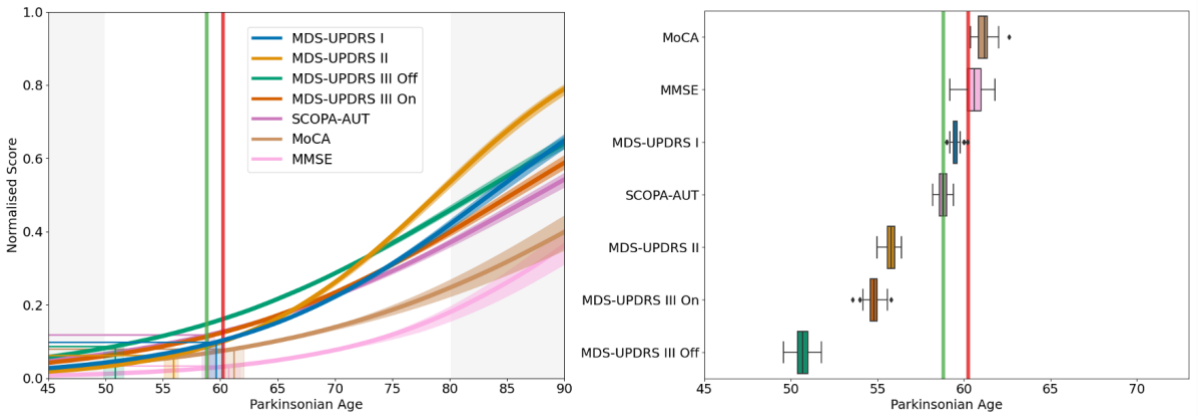

Supplementary Figure 5: Typical PD progression of the 8 clinical endpoints on the clinical disease course map. The clinical disease course map was trained on PD data from PPMI, ICEBERG and DIGPD. Left panel: the progression of the endpoints from the most typical normal value (0) to the maximum pathological change (1) with Parkinsonian age is shown. Shaded areas around the curves correspond to the 95% confidence interval. Transparent regions show the range of PA where the curves are informed by less than 5% of the data. Right panel: the time points at which endpoints become abnormal is shown with 95% confidence intervals. Vertical lines indicate the estimated Parkinsonian age at first symptoms (light red) and PD diagnosis (dark red).